ACS APPLIED MATERIALS & INTERFACES

Research Article

www.acsami.org

Tuning Surface Charge and Morphology for the Efficient Detection of Dopamine under the Interferences of Uric Acid, Ascorbic Acid, and Protein Adsorption

Chien-Hsun Chen[†] and Shyh-Chyang Luo*[,†,‡]

[†]Department of Materials Science and Engineering, National Cheng Kung University, 1 University Road, Tainan 70101, Taiwan

[‡]Department of Materials Science and Engineering, National Taiwan University, No. 1, Sec. 4, Roosevelt Road, Taipei, 10617 Taiwan

Supporting Information

ABSTRACT: In this research, we aimed to evaluate the impact of the surface charges and morphologies of electrodes on electrochemically detecting dopamine (DA) in the presence of protein adsorption, uric acid (UA), and ascorbic acid (AA). Through the electropolymerization of functionalized 3,4-ethylenedioxythiophenes (EDOT) directly on Au electrodes, we successfully created PEDOT-coated electrodes with three different functional groups and nanostructures. Negatively charged carboxylic acid groups attracted DA while reducing the interferences of UA and AA due to electrostatic effect. We used charge-free tetra(ethylene glycol) and zwitterionic phosphocholine groups are used to evaluate the interference of protein adsorption on DA sensing because they both can effectively prevent the nonspecific adsorption of proteins. These two electrodes can avoid protein adsorption, yet proved ineffective for DA sensing: both tetra(ethylene glycol) and the phosphocholine groups are electroneutral and have minimal electrostatic interactions with DA. We also used three proteins of different isoelectric points - bovine serum albumin, lysozyme, and fibrinogen - to evaluate the influence of protein adsorption on DA detection. We found that for an electrode coated with carboxylic acid-functionalized PEDOT, the adsorption of positively charged lysozyme can promote the detection sensitivity of AA and UA, and that all protein adsorption lowers the sensitivity of DA. In contrast, nanostructures promote the detection sensitivity of all three molecules. All of our tested functionalized PEDOT-coated electrodes demonstrated good stability and functionality in buffers.

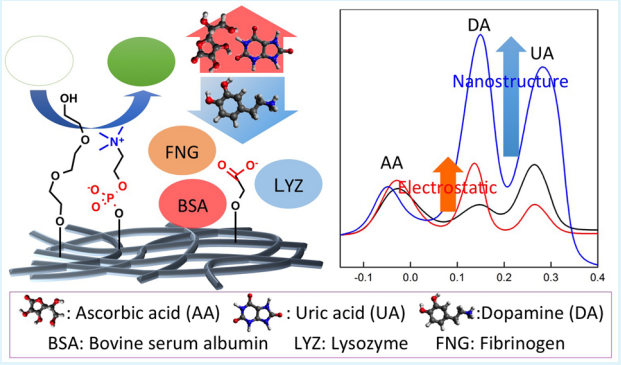

KEYWORDS: *dopamine electrochemical detection, conducting polymer, electrostatic effect, nanostructure, nonspecific adsorption, nonfouling surface*

INTRODUCTION

Serving to allow communication between neuron cells, the neurotransmitter dopamine (DA) is critical in human brains and plays an important role in several important diseases of the nervous system, such as Parkinson's disease and schizophrenia.[1,2] Therefore, for clinical trials to develop new technologies and reliable platforms, precise measurement and monitoring of DA concentration in biological systems are worth pursuing. Over the past few decades, researchers have thoroughly studied the in vivo monitoring of the concentration of dopamine in brains or small organs.[3] Generally, the application electroanalytical techniques to detect DA directly in vivo is one full of challenges. The first challenge is to avoid interferences from non-DA biomolecules with oxidation potentials similar to those of DA. The typical examples are ascorbic acid (AA) and uric acid (UA). New electrode materials, such as graphene[4,5] and carbon nanotubes,[6,7] as well as various surface modification approaches, including self-assembly monolayers[8,9] and polymer coatings,[10,11] have been developed to overcome this challenge.

Another challenge is the fabrication of microsize electrodes for use in conducting electrochemical experiments in vivo or for small organs. Presently, the most commonly used microelectrodes are carbon-based electrodes. These electrodes possess several advantages, including low cost, wide electrochemical windows, and moderate electrocatalytic activities for a variety of redox reactions.[12] The discovery of new types of carbon nanostructures has further expanded the potential applications of carbon-based electrodes.[13,14] Researchers also successfully used carbon fibers as electrodes for implantable electrochemical DA sensors.[15,16] The requirements of high spatial and temporal resolution are two other challenges scholars confront in in vivo DA monitoring.[17]

One critical issue for electrodes used in biological environments is the adsorption of proteins. The adsorption of proteins

Received: July 20, 2015
Accepted: September 18, 2015
Published: September 18, 2015

DOI: 10.1021/acsami.5b06526
ACS Appl. Mater. Interfaces 2015, 7, 21931−21938

not only lowers the sensitivity of the electrodes, but also causes the failure of chronically implanted electrodes for the in vivo monitoring of DA.[18] Currently, the most efficient way to prevent the nonspecific binding of proteins is to make surfaces hydrophilic enough to retain a thin water layer on surfaces.[19,20] Poly(ethylene glycol) (PEG) and oligo(ethylene glycol)-based coating have been the key candidate for this purpose, and PEG has been used in various bioengineering applications, including drug delivery,[21] tissue engineering,[22,23] and biochips.[24] Over the past decade, several alternatives have been developed, including zwitterionic phosphorylcholine[25−27] and betaine[28,29] groups. The zwitterionic groups show strong interaction with water molecules and also efficiently resist nonspecific protein adsorption.[30,31] Despite the advances in development of the nonfouling surfaces during these years, few studies explore the possibility of using nonfouling coatings on electrodes used for long-term in vivo DA detection. Overall, the studies that evaluate the influence of protein adsorption on DA detection were limited; we currently stand without a systematic study of this phenomenon.

In this study, we analyzed correlation between the selective DA sensing, protein adsorption, and surface properties of electrodes, including surface charge and morphologies. Using poly(3,4-ethylenedioxythiophene)-coated electrodes of various surface functional groups and nanostructures, we evaluated DA sensing in the presence of protein adsorption, uric acid, and ascorbic acid. Poly(3,4-ethylenedioxythiophene) or PEDOT has been proven an effective electrode material with superior stability in a biological buffer.[32,33] Previous work has demonstrated the applications of PEDOT-based composites, including Au nanoparticles, graphene oxide, and Nafion, as electrodes for DA sensing.[34−36] During the past few years, we have been developing PEDOT with various functional groups as conductive biointerfaces.[37] Carboxylic acid-functionalized EDOT (EDOT-COOH) gave polymer films with stored specific charges higher than those of PEDOT.[38] Polystyrene beads coated with poly(EDOT-COOH) showed a measured zeta-potential of −52.11 mV, which indicates a negatively charged surface.[39] As for oligo(ethylene glycol)-functionalized EDOT (EDOT-EG_n)[40] and the zwitterionic phosphocholine-functionalized EDOT (EDOT-PC),[41−43] both can effectively prevent the nonspecific adsorption of proteins. In the present study, poly(EDOT-COOH) was used for the purpose of selective DA detection due to the electrostatic effect. Poly(EDOT-EG_4) and poly(EDOT-PC) were used to evaluate the influence of protein binding on DA detection. The application of functionalized PEDOTs allows us to precisely control the surface properties of electrodes, while the covalent bonding between functional groups and PEDOTs ensures the stability of these functionalized PEDOT-coated electrodes. Furthermore, by tuning the electropolymerization processes, we were able to synthesize both smooth and nanostructured PEDOT films, gaining the ability to simultaneously evaluate the influence of surface morphologies on DA detection.

EXPERIMENTAL SECTION

Chemicals and Reagents. 3,4-Ethylenedioxythiophene (EDOT) and hydroxymethyl EDOT (EDOT-OH) were purchased from Sigma-Aldrich and used without further purification. EDOT-COOH and EDOT-EG_4 were synthesized following procedures previously reported.[40,44] In short, for EDOT-COOH, EDOT-OH (861 mg, 5.0 mmol), NaI (150 mg, 1.0 mmol), and NaH (60% suspension in mineral oil, 240 mg, 6.0 mmol) were added into a round-bottom flask a stir bar. The flask was then charged with N_2. After dry THF (20 mL) was added into the flask, the suspension was stirred for 15 min and cooled in an ice bath. Methyl bromoacetate (0.57 mL, 0.92 g, 6.0 mmol) was added slowly, and the reaction mixture was stirred for 18 h. The majority of THF was removed with a rotavap; the crude product was partitioned between water and ethyl acetate, and the aqueous layer was extracted with ethyl acetate. The combined organic layers were washed with brine, dried with $MgSO_4$, and evaporated. After being purified with a silica gel column (hexane/ethyl acetate = 5:1), the product (610 mg) was dissolved in THF (10 mL) in a 100 mL round-bottom flask. After aqueous NaOH solution (2 M, 10 mL) was added, the mixture was stirred vigorously until the starting material was completely consumed, which was confirmed by thin layer chromatography. The mixture was acidified to pH < 3 using HCl and then extracted with ethyl acetate. The combined organic layers were washed with water, dried ($MgSO_4$), and evaporated. EDOT-COOH (480 mg, 63%) was obtained. ^{1}H NMR ($CDCl_3$): δ 6.36 (d, 2H, J = 3.6 Hz), 6.34 (d, 1H, J = 3.6 Hz), 4.38 (ddd, 1H, J = 11.6, 7.2, 2.4 Hz), 4.26 (dd, 1H, J = 11.6, 2.4 Hz), 4.24 (s, 2H), 4.12 (dd, 1H, J = 11.6, 7.2 Hz), 3.85 (dd, 1H, J = 10.4, 4.8 Hz), 3.81 (dd, 1H, J = 10.4, 4.8 Hz). ^{13}C NMR ($CDCl_3$): δ 175.2, 141.3, 141.1, 100.0, 99.9, 72.6, 70.0, 68.4, 65.8. HRMS (FAB): [M + H] calcd for $C_9H_{11}O_5S$, 231.0237; found, 231.0237. For EDOT-EG_4: Trityl chloride (5.58 g) was dissolved in a mixture of tetraethylene glycol (17.2 mL) and dichloromethane (30 mL). After pyridine (1.6 mL) was added, the mixture was stirred overnight, then diluted with dichloromethane and washed with H_2O. To the solution, a stir bar and triethylamine (4 mL) were added, and the flask was cooled at 0 °C and mesyl chloride (2.3 mL) added dropwise. After being stirred overnight, the reaction was quenched with H_2O, washed with saturated $NaHCO_3$, dried over $MgSO_4$, and purified by chromatograph. In a 300 mL flask EDOT-OH (5.41g), NaI (0.471 g) and a stirrer were sealed and backfilled with N_2. Dried DMF (40 mL) and 1.88 g NaH were added under N_2 flow. After the mixture was stirred for 15 min, a solution of 16.25 g product in DMF (40 mL) was added. The whole mixture was stirred overnight. The solution was then poured into 200 mL ethyl acetate and washed with 150 mL H_2O for 5 times. The solvent was removed by a rotavapor, and the residue dispersed in methanol (400 mL) with Amberlite (40 g). After being stirred at 70 °C and refluxed over 6 h, the resin was filtered and purified by chromatography. ^{1}H NMR ($CDCl_3$): δ 6.33 (s, 2H), 4.34 (m, 1H), 4.26 (dd, J = 11.6, 2.4 Hz, 1H), 4.07 (dd, J = 11.6, 7.6 Hz, 1H), 3.79−3.66 (m, 16H), 3.61 (m, 2H), 2.42 (broad s, 1H). ^{13}C NMR ($CDCl_3$): δ 141.5, 141.4, 99.7, 99.6, 72.6, 72.5, 71.1, 70.7, 70.6, 70.5, 70.4, 70.3, 69.6, 66.1, 61.7. HRMS (FAB): Calcd for $C_{15}H_{25}O_6S$ ($[M + H]^+$): 349.1277. Found: 349.1269. EDOT-PC was obtained from Dr. Hsiao-hua Yu, which had been prepared following procedures previously reported.[41] Chemical reagents, including dioctyl sulfosuccinate sodium salt (DSS), sodium dodecyl sulfate (SDS), lithium perchlorate ($LiClO_4$), tetrabutylammonium perchlorate (TBAP), and organic solvents, including acetonitrile (CH_3CN) and dichloromethane (CH_2Cl_2) were purchased from Sigma-Aldrich and used without further purification. Biological reagents, including bovine serum albumin (BSA), lysozyme (LYZ), fibrinogen (FNG), and PBS buffer were also obtained from Sigma-Aldrich.

Fabrication of PEDOT Electrodes. The electropolymerization was performed by using a potentiostat (PGSTAT101, Autolab). Smooth PEDOT films were deposited on Au electrodes from aqueous solutions containing 10 mM EDOT, 100 mM $LiClO_4$ and 50 mM of SDS by applying cyclic potential (−0.6 to 1.1 V vs Ag/AgCl at a scan rate of 100 mV s^{-1}). Nanostructured PEDOT films were fabricated by electropolymerization using a constant voltage (1.1 V vs Ag/Ag^+) for 20 s. EDOT solutions were prepared by dissolving monomers at a concentration of 10 mM in CH_2Cl_2 containing 100 mM TBAP as electrolyte. The electrochemical cell was immersed into a 0 °C bath for at least 3 min before performing electropolymerization. EDOT-EG_4, EDOT-PC and EDOT-COOH were electropolymerized on smooth or nanostructured PEDOT from 0.01 M solutions in CH_3CN containing 50 mM DSS and 100 mM $LiClO_4$ by applying cyclic potential as described previously.

DOI: 10.1021/acsami.5b06526
ACS Appl. Mater. Interfaces 2015, 7, 21931−21938

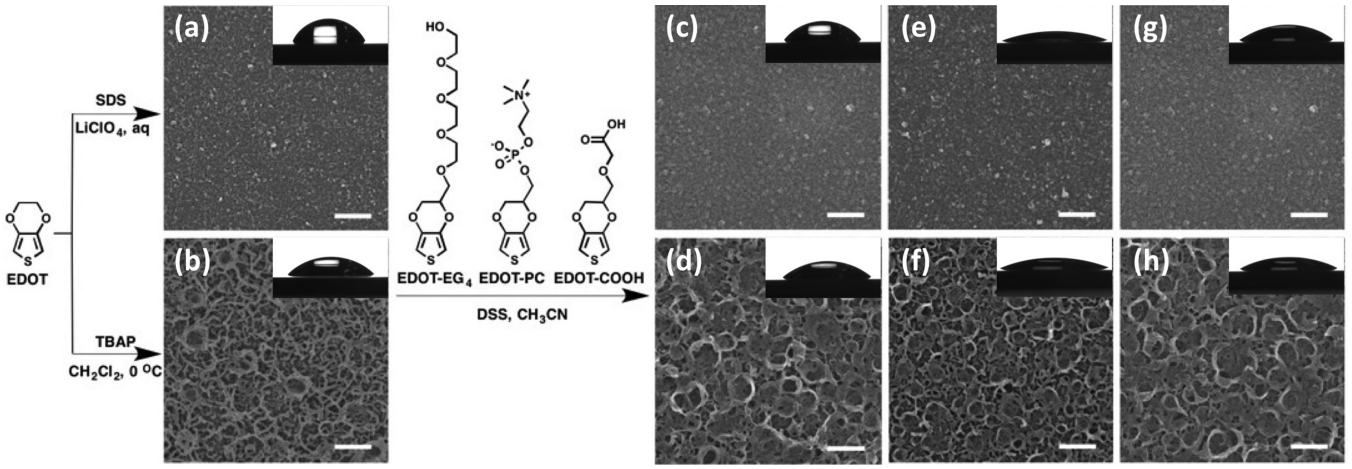

Figure 1. Synthesis procedure and SEM images of smooth and nanostructured PEDOT, poly(EDOT-EG_4), poly(EDOT-PC), and poly(EDOT-COOH): (a) Smooth PEDOT prepared by electropolymerization in aqueous solutions in the presence of SDS and LiClO4; (b) Nanostructured PEDOT prepared by electropolymerization in CH_2Cl_2 containing TBAP; (c) Smooth poly(EDOT-EG_4) and (d) nanostructured poly(EDOT-EG_4); (e) smooth poly(EDOT-PC); and (f) poly(EDOT-PC); (g) smooth poly(EDOT-COOH); and (h) nanostructure poly(EDOT-COOH) prepared by electropolymerization in CH_3CN solutions in the presence of DSS by using smooth PEDOT and nanostructured PEDOT as hard templates. (Scale bar = 500 nm).

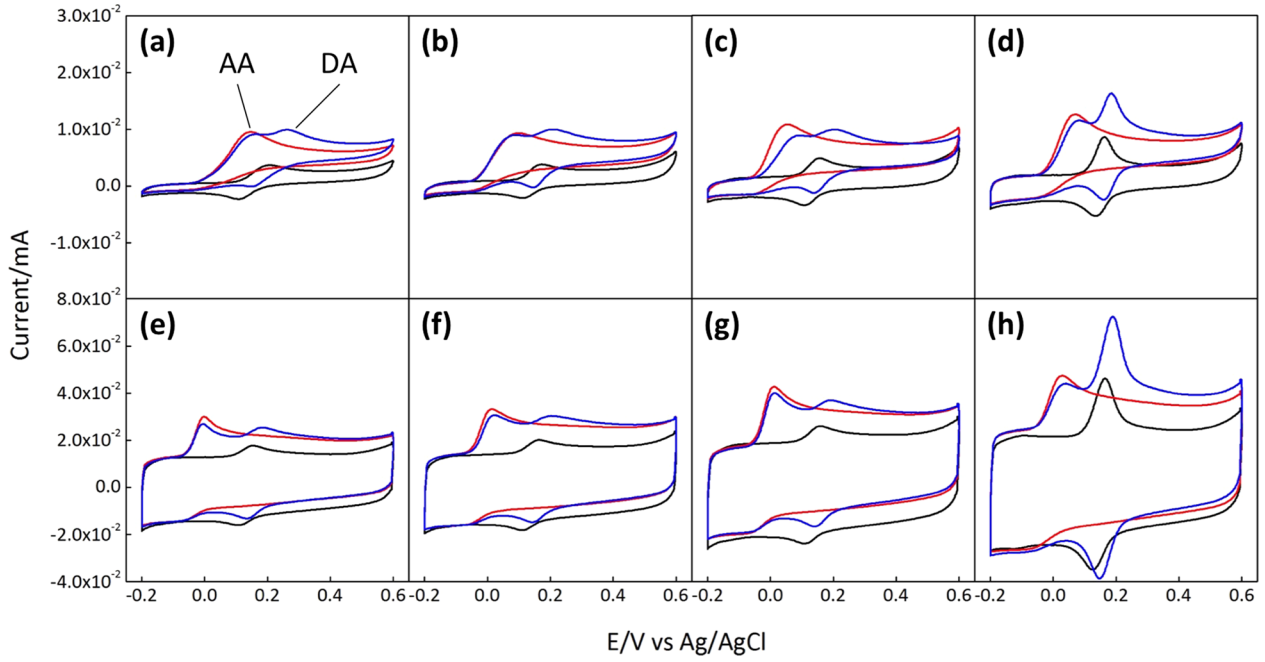

Figure 2. Cyclic voltammograms of various functionalized PEDOT-coated electrodes in PBS buffer containing 0.1 mM DA (—, black line); containing 1 mM AA (—, red line); containing both 0.1 mM DA and 1 mM AA (—, blue line) by applying cyclic potentials from −0.2 to 0.6 V (vs Ag/AgCl) at rate of 100 mV s^{-1}. PEDOT-coated electrodes include smooth (a) PEDOT, (b) poly(EDOT-EG_4), (c) poly(EDOT-PC), and (d) poly(EDOT-COOH) compared to nanostructured (e) PEDOT, (f) poly(EDOT-EG_4), (g) poly(EDOT-PC), and (h) poly(EDOT-COOH).

Characterization of PEDOT Morphology and Surface Properties. The surface morphology of PEDOT electrodes was examined with field emission scanning electron microscopy (FESEM). FESEM was performed with a HITACHI SU8000 at a vacuum of 10^{-10} Torr and an accelerating voltage of 5 kV. Static contact angle of water (~1 μL) was performed by using a contact angle measurement system (Model 100SB, Sindatek) at room temperature. Protein binding was studied by QCM-D measurement, which is performed by Q-Sense system (Biolin Scientific) to monitor the interactions between proteins and functionalized PEDOT substrates. The protein concentrations of bovine serum albumin, lysozyme and fibrinogen were 1 mg/mL. The PEDOTs were electropolymerized on the surface of a Au sensor crystal (QSX 301, Biolin Scientific). The frequency changes in the third overtone are used to estimate the protein adsorption in mass/area.

Electrochemical Characterization. All electrochemical measurements were performed in a glass cell integrated with an Autolab PGSTAT101 potentiostat. A Ag/AgCl and a Pt electrode were used as reference and counter electrodes, respectively. Cyclic voltammetric (CV) measurements were performed in PBS buffer over the potential ranging from −0.2 to 0.6 V vs Ag/AgCl at a scan rate of 100 mV s^{-1}. To record the differential pulse voltammograms (DPV), the following input parameters were used: potential rage from −0.15 to 0.4 V vs Ag/AgCl at a scan rate of 4 mV s^{-1}. A pulse with 50 mV amplitude, 50 ms width, 500 ms interval and quiet time of 30 s was applied. Peak currents were determined by subtraction of a manually added baseline.

DOI: 10.1021/acsami.5b06526
ACS Appl. Mater. Interfaces 2015, 7, 21931−21938

RESULTS AND DISCUSSION

Functionalized PEDOT Electrodes and Their Surface Properties. To fabricate the functionalized PEDOT electrode of two different surface morphologies, we applied the electropolymerization of PEDOT in two solution systems, as shown in Figure 1.

The electropolymerization of PEDOT on an Au electrode in aqueous solutions containing 50 mM sodium dodecyl sulfate (SDS) resulted in smooth PEDOT surfaces of roughness usually less than 10 nm (Figure 1a). When synthesizing PEDOT by electropolymerization in CH_2Cl_2 solutions containing tetrabutylammonium persulfate (TBAP) as electrolytes, we found PEDOT to form fiber-type nanostructures as shown in Figure 1e. We then used these two surfaces as our hard templates to synthesize functionalized PEDOT by the electropolymerization of three functionalized EDOTs—EDOT-EG_4, EDOT-PC, and EDOT-COOH—in CH_3CN solutions containing dioctyl sodium sulfosuccinate (DSS). By this method, we successfully created both smooth and nanostructured poly(EDOT-EG_4), poly(EDOT-PC), and poly(EDOT-COOH), as shown in Figure 1c–h. Compared to water contact angles of smooth PEDOT surfaces, the contact angles after the coating with poly(EDOT-EG_4), poly(EDOT-PC), and poly(EDOT-COOH) were small. More hydrophilic surfaces appeared due to the contribution of tetra(ethylene glycol), phosphocholine, and carboxylic acid groups. Poly(EDOT-PC) offered the lowest water contact angle, and poly(EDOT-EG_4) presented a high contact angle compared to those of poly(EDOT-PC) and poly(EDOT-COOH). In contrast, the water contact angle of the nanostructured PEDOT film was lower than the smooth PEDOT film, a fact that stems from the nanostructure effect amplifying the surface properties[44,45] The other functionalized PEDOT films also showed similar trends. We also used X-ray photoelectron spectroscopy (XPS) to confirm the chemical compositions of PEDOT and functionalized PEDOT films, as shown in Supporting Information (SI) S1. After the electropolymerization of poly(EDOT-COOH) on PEDOT substrates, we witnessed a strong C 1s peak at 287 eV. This corresponded to carbonyl bonding from carboxylic acid groups. N 1s and P 2p peaks were only observed after poly(EDOT-PC) was electropolymerized on PEDOT substrates.

Electrostatic Interaction and the Nanostructure Effect on DA Detection. The cyclic voltammograms of various functionalized PEDOT-coated Au electrodes in PBS buffer in the presence of sole 0.1 mM DA, sole 1 mM AA, or both 0.1 mM DA and 1 mM AA were shown in Figure 2.

Before the PEDOT films were coated on the Au electrodes, the oxidation peaks of DA and AA could not resolve, as shown in SI S2. After the PEDOT films coated Au electrodes, the oxidation peaks of AA and DA resolved, and the peak position resolved, depending on the functional groups and surface morphology of PEDOT coating. Compared to the oxidation peak of DA measured by electrodes coated with smooth PEDOT (Figure 2a), smooth poly(EDOT-EG_4) (Figure 2b), and smooth poly(EDOT-PC) (Figure 2c), the current intensity of DA oxidation peak measured by the electrode coated with smooth poly(EDOT-COOH) (Figure 2d) was high. Hence, the negative charges on the poly(EDOT-COOH) films successfully enhanced detection through the electrostatic interaction with DA. The oxidation peaks of AA did not show obvious change when electrodes of different functionalized PEDOT coating were applied. Yet the surface morphology of PEDOT-coated electrodes played an important role in the creation of AA's oxidation peaks. Compared to the oxidation potential of AA as measured by all electrodes coated with smooth PEDOT, the oxidation potential of AA measured via nanostructured PEDOT-coated electrodes was significantly lower. This result might be due to a positively charged PEDOT backbone at its doping state. The nanostructure seemed to enhance the charge effect, which is beneficial to the oxidation of negatively charged AA and lowers the oxidation potential. The nanostructured poly(EDOT-COOH) provided a larger surface area than the one delivered by smooth poly(EDOT-COOH) and interacted with more DA in the solutions. The oxidation peak area measured by an electrode coated with nanostructured poly(EDOT-COOH) was three times higher than that of an electrode coated with smooth poly(EDOT-COOH).

Variations of Protein Binding on PEDOT-Coated Electrodes. We used a quartz crystal microbalance with dissipation (QCM-D) system to evaluate the protein binding on our PEDOT and functionalized PEDOT films, the results of which are summarized as shown in Figure 3.

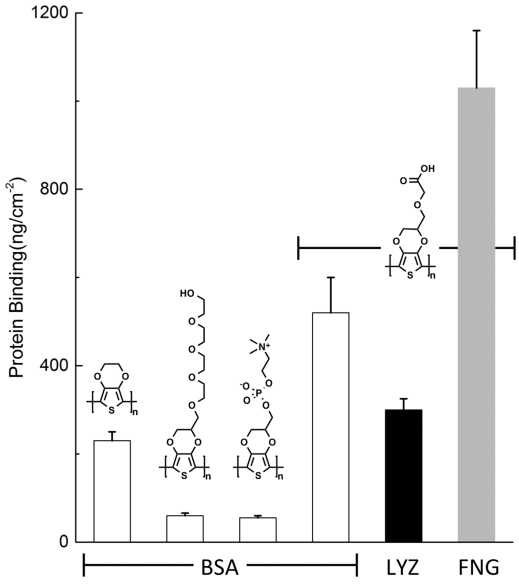

Figure 3. Comparison of bovine serum albumin (BSA, white) binding on PEDOT, poly(EDOT-EG_4), poly(EDOT-PC), and poly(EDOT-COOH). Binding of lysozyme (LYZ, black) and fibrinogen (FNG, light gray) on poly(EDOT-COOH). The concentration of three proteins for binding study by QCM-D was 1 mg/mL.

First, we tested the binding of bovine serum albumin (BSA) on various functionalized PEDOTs. The isoelectric point (p*I*) of BSA is 4.7, which indicates a totally negatively charged status of BSA. Compared to PEDOT and poly(EDOT-COOH), poly(EDOT-EG_4) and poly(EDOT-PC) showed much weaker binding to bovine serum albumin (BSA). The results revealed that the hydrophilic tetra(ethylene glycol) and phosphocholine groups can effectively prevent the nonspecific binding of BSA. Compared to PEDOT, poly(EDOT-COOH) showed a notably higher binding of BSA. The negatively charged surfaces of poly(EDOT-COOH) could hardly repulse BSA effectively. The contribution of the interactions of specific carboxylic group binding site in BSA played a role in this result.[46] We further tested the binding of lysozyme (LYZ) and fibrinogen (FNG) on poly(EDOT-COOH). LYZ (p*I* = 11.35) is positively

DOI: 10.1021/acsami.5b06526
ACS Appl. Mater. Interfaces 2015, 7, 21931–21938

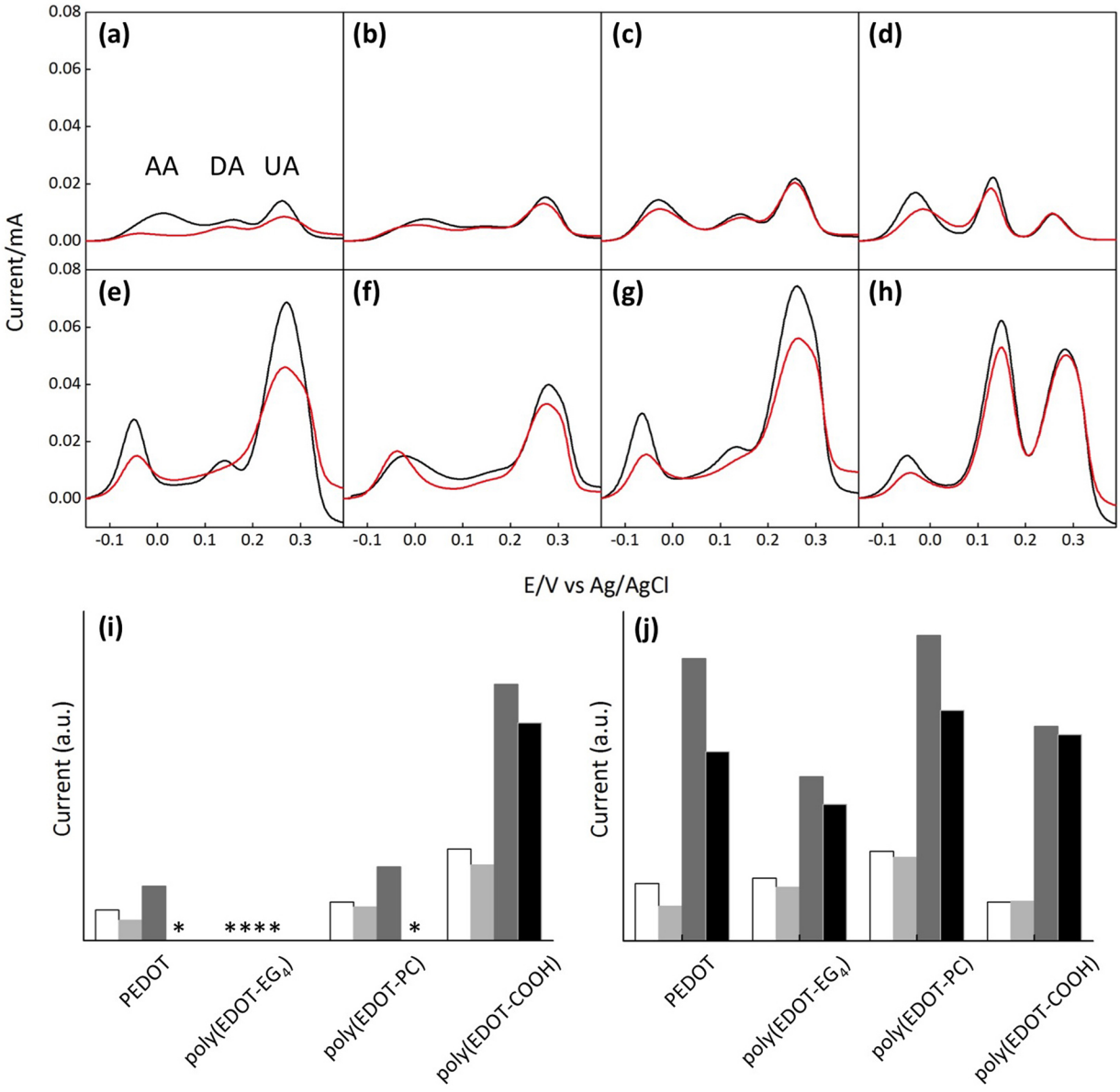

Figure 4. Differential pulse voltammetry (DPV) response at electrodes coated with smooth (a) PEDOT, (b) poly(EDOT-EG4), (c) poly(EDOT-PC), and (d) poly(EDOT-COOH) compared to electrodes coated with nanostructured (e) PEDOT, (f) poly(EDOT-EG4), (g) poly(EDOT-PC), and (h) poly(EDOT-COOH) in PBS buffer containing 1 mM AA, 0.1 mM DA, and 0.2 mM UA before (—, black line) and after (—, red line) BSA binding; Current readout of (i) DA and (j) UA measured by electrodes coated with smooth films (white), smooth films after BSA binding (light gray), nanostructured films (gray), and nanostructured films after BSA binding (black). *Peaks not clearly resolved.

charged, and FNG (p*I* = 5.2) is slightly negatively charged in a PBS buffer of pH = 7.4. Nevertheless, the results confirmed strong nonspecific bindings of both LYZ and FNG on poly(EDOT-COOH), indicating that neither the isoelectric point of proteins nor the net charge of proteins are a decisive factor in determining whether the proteins can be nonspecifically adsorbed on our PEDOT platforms.

DA Detection under the Interferences of AA, UA, and BSA Binding. We evaluated the interferences of AA, UA, and protein binding by applying differential pulse voltammetry (DPV) measurement on various PEDOT-coated electrodes, as shown in Figure 4.

The DPV was conducted in a PBS buffer containing 1 mM AA, 0.1 mM DA, and 0.2 mM UA. Compared to the electrodes coated with smooth PEDOT (Figure 4a), poly(EDOT-EG_4) (Figure 4b), or poly(EDOT-PC) (Figure 4c), the DPV by the electrode coated with poly(EDOT-COOH) (Figure 4d) showed strong oxidation peak of DA at ∼0.15 V vs Ag/AgCl. The oxidation of AA (∼−0.01 V vs Ag/AgCl) and UA (∼0.29 V vs Ag/AgCl) were resolved on all PEDOT-coated electrodes. Compared to that of the smooth PEDOT-coated electrodes, the DPV measured by nanostructured PEDOT-coated electrodes (Figure 4e−h) generally showed much higher current readout for the oxidation peaks. To test the interferences of protein binding, we allowed the adsorption of proteins by immersing electrodes into a PBS buffer containing 1.0 mg/mL BSA overnight. The electrodes were rinsed with the PBS buffer before the DPV measurements. After the PEDOT-coated electrode was blocked by BSA, the measured peak currents were generally lower than before protein binding, a result indicating that BSA adsorption interferes with the oxidation of AA, DA, and UA. For a better understanding and comparison

DOI: 10.1021/acsami.5b06526
ACS Appl. Mater. Interfaces 2015, 7, 21931−21938

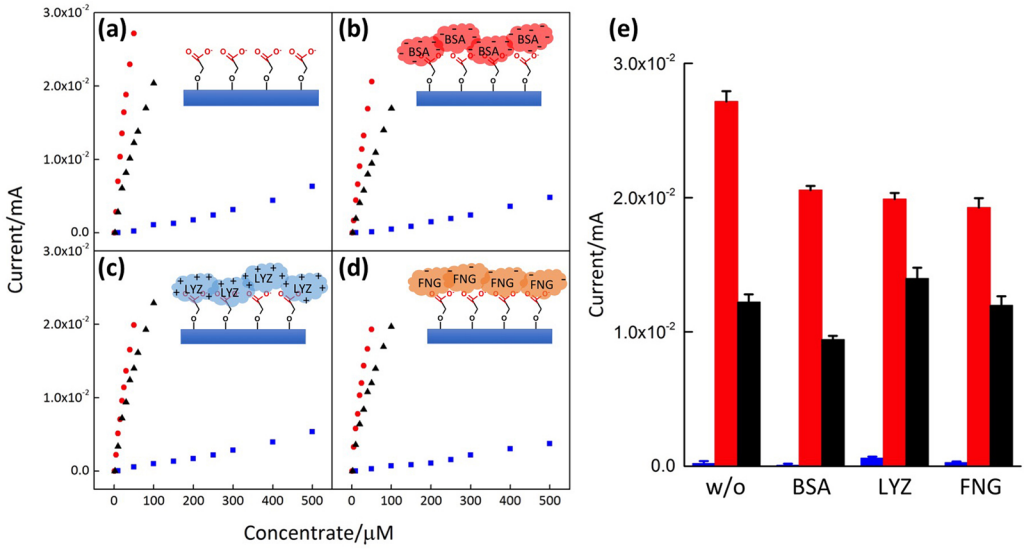

Figure 5. Current−concentration relationship of DA (●, red circle), UA (▲, black triangle), AA (■, blue square) measured by (a) bare nanostructured poly(EDOT-COOH)-coated electrode, and nanostructured poly(EDOT-COOH)-electrodes after (b) BSA binding, (c) LZY binding, and (d) FNG binding. (e) The current readout of DA (red), UA (black), and AA (blue) when [AA] = [DA] = [UA] = 50 μM.

of these measurements, we present the current readouts of the DA oxidation peaks and UA oxidation peaks in Figure 4i and Figure 4j, respectively. Compared to the electrode coated by smooth PEDOT, the electrodes coated with smooth poly(EDOT-EG_4) and smooth poly(EDOT-PC) showed less of a current drop after the BSA binding, which indicates the interference due to protein binding was not significant for poly(EDOT-EG_4) or poly(EDOT-PC), whereas it was for PEDOT. This result is coincident to a protein-binding measurement using a QCM-D system. Most importantly, only poly(EDOT-COOH)-coated electrodes showed strong DA oxidation peaks, even when the electrode surfaces were blocked by BSA (Figure 4i). The binding of BSA reduces the current signal by 15 to 20% in general. Nanostructures increased the detection sensitivity of UA, as shown in Figure 4j, and the binding of BSA also limited the oxidation of UA on PEDOT-coated electrodes. On the basis of these results, we realized the negatively charged carboxylic acid to be the key factor for DA detection. Although the EG_4 and PC groups were useful to prevent the nonspecific binding of proteins, our results showed an electrostatic interaction dominating the sensing event. We also tested the performance of copolymer of poly(EDOT-COOH) and poly(EDOT-PC), as shown in SI S3. The results showed that even a 50% feed ratio of EDOT-PC causes a significant drop in the DA oxidation signal.

The Protein Charge Effect, Concentration Dependence, and Stability. We further evaluated the current-concentration dependence of nanostructured poly(EDOT-COOH)-coated electrodes using a DPV method, as shown in SI S4 and S5. The test was also evaluated under the binding of various proteins, including BSA, LZY, and FNG. The data are summarized and shown in Figure 5.

As shown in Figure 5a−d, the electrodes coated with nanostructured poly(EDOT-COOH) resulted in a nearly linear relationship for DA (1 to 50 μM), AA (10 to 500 μM), and UA (2 to 100 μM), regardless of whether measured before or after protein binding. On the basis of the slope of the current−concentration relationship, we found these electrodes to provide the highest sensitivity to DA and a minimum sensitivity to AA. To clearly illustrate the influence of protein binding on the sensing of AA, DA, and UA, we compared the current readout when the three chemicals were at same concentration of 50 μM as shown in Figure 5e. The current readouts of DA signals significantly decreased after protein binding, indicating that the binding of proteins on poly(EDOT-COOH) interferes with the electrostatic interaction between DA and carboxylic acid groups. Remarkably, the current readouts of AA and UA signals increased after LYZ binding, implying a higher sensitivity of AA and UA. This is due to the electrostatic interaction between acids and positively charged LYZ.

We also evaluated the stability of the poly(EDOT-COOH)-coated electrodes, as shown in SI S6. The DPV results were obtained after the electrodes were immersed into a PBS buffer in the presence of BSA for 30 days. The current readout from the freshly prepared poly(EDOT-COOH)-coated electrode, as shown in Figure 5b, nearly matched the current readout from the same electrode after 30-day immersion in the PBS buffer. This indicates a good stability for PEDOT-coated electrodes.

■ CONCLUSIONS

We studied PEDOT-coated electrodes for dopamine (DA) sensing under the interferences of ascorbic acid (AA), uric acid (UA), and protein adsorption. Our examination provides information pertinent to making electrodes used for in vivo monitoring purposes. We focused PEDOT-coated electrodes with three different functional groups, including tetra(ethylene glycol), phosphocholine, and carboxylic acid groups. Although coating electrodes with charge-free tetra(ethylene glycol) and zwitterionic phosphocholine groups on the surface can prevent nonspecific protein adsorption on electrodes, these two coatings failed to provide sensitive DA detection due to their weak electrostatic interactions with DA. In contrast, electrodes with carboxylic acid groups provided a significant enhancement in DA detection, even when the surfaces were blocked by proteins. Furthermore, these groups reduced the interference of AA and UA. These results indicate that the electrostatic interaction between carboxylic acid groups and DA dominates the sensing events, even under the interference of protein

DOI: 10.1021/acsami.5b06526
ACS Appl. Mater. Interfaces 2015, 7, 21931−21938

adsorption. Compared to smooth PEDOTs, the nanostructured PEDOTs not only enhance the detection sensitivity of DA, but also that of both AA and UA. This might be due to the positively charged backbones of PEDOTs at their doping states, as positively charged backbones can attract negatively charged AA and UA. The protein adsorption generally lowers the detection sensitivity of DA due to the hindrance of the electrostatic interaction between DA and the carboxylic acid groups on electrodes. Notably, after the adsorption of LZY on poly(EDOT-COOH), the detection sensitivity of AA and UA was slightly promoted. This observation entails the possibility of protein adsorption being used for surface modifications, modifying the detection sensitivity by tuning electrostatic interaction with targeted molecules. Overall, our study provides some insights into the working influence of surface charge and surface morphology on DA detection, especially in the presence of protein adsorption. Although protein adsorption reduces the sensitivity of electrodes for DA detection, nonfouling coatings, such as tetra(ethylene glycol) and phosphocholine, might not be applicable due to their low sensitivity in detecting DA. The adsorption of proteins might alter the electrode sensitivity on DA, AA, and UA due to the electrostatic interaction between the proteins and these charged molecules.

■ ASSOCIATED CONTENT

Supporting Information

The Supporting Information is available free of charge on the ACS Publications website at DOI: 10.1021/acsami.5b06526.

XPS spectrum of functionalized PEDOT electrodes, cyclic voltammograms of Au and copolymer electrodes, differential pulse voltammograms of PEDOT-coated electrodes in the presence of protein binding, and stability test (PDF)

■ AUTHOR INFORMATION

Corresponding Author

*E-mail: shyhchyang@ntu.edu.tw (S.-C.L.).

Author Contributions

The manuscript was written through contributions of all authors. All authors have given approval to the final version of the manuscript.

Notes

The authors declare no competing financial interest.

■ ACKNOWLEDGMENTS

The monomer EDOT-PC was provided by the courtesy of Dr. Hsiao-hua Yu from Institute of Chemistry at Academia Sinica, Taiwan. We gratefully acknowledge the financial support provided by the Ministry of Science and Technology of Taiwan under grant NSC 102-2113-M006-013-MY2 and Academia Sinica under grant AS-104-TP-A11.

■ REFERENCES

(1) Dawson, T. M.; Dawson, V. L. Molecular Pathways of Neurodegeneration in Parkinson's Disease. *Science* **2003**, *302*, 819–822.

(2) Lodge, D. J.; Grace, A. A. Aberrant Hippocampal Activity Underlies the Dopamine Dysregulation in an Animal Model of Schizophrenia. *J. Neurosci.* **2007**, *27*, 11424–11430.

(3) Wightman, R. M.; May, L. J.; Michael, A. C. Detection of Dopamine Dynamics in the Brain. *Anal. Chem.* **1988**, *60*, 769A–779A.

(4) Zhou, M.; Zhai, Y. M.; Dong, S. J. Electrochemical Sensing and Biosensing Platform Based on Chemically Reduced Graphene Oxide. *Anal. Chem.* **2009**, *81*, 5603–5613.

(5) Kuila, T.; Bose, S.; Khanra, P.; Mishra, A. K.; Kim, N. H.; Lee, J. H. Recent Advances in Graphene-Based Biosensors. *Biosens. Bioelectron.* **2011**, *26*, 4637–4648.

(6) Zhao, J.; Zhang, W.; Sherrell, P.; Razal, J. M.; Huang, X.-F.; Minett, A. I.; Chen, J. Carbon Nanotube Nanoweb-Bioelectrode for Highly Selective Dopamine Sensing. *ACS Appl. Mater. Interfaces* **2012**, *4*, 44–48.

(7) Huang, Y.; Miao, Y.-E.; Ji, S.; Tjiu, W. W.; Liu, T. Electrospun Carbon Nanofibers Decorated with Ag-Pt Bimetallic Nanoparticles for Selective Detection of Dopamine. *ACS Appl. Mater. Interfaces* **2014**, *6*, 12449–12456.

(8) Raj, C. R.; Ohsaka, T. Voltammetric Detection of Uric Acid in the Presence of Ascorbic Acid at a Gold Electrode Modified with a Self-Assembled Monolayer of Heteroaromatic Thiol. *J. Electroanal. Chem.* **2003**, *540*, 69–77.

(9) Matos, I. d. O.; Alves, W. A. Electrochemical Determination of Dopamine Based on Self-Assembled Peptide Nanostructure. *ACS Appl. Mater. Interfaces* **2011**, *3*, 4437–4443.

(10) Wang, H. S.; Li, T. H.; Jia, W. L.; Xu, H. Y. Highly Selective and Sensitive Determination of Dopamine Using a Nafion/Carbon Nanotubes Coated Poly(3-methylthiophene) Modified Electrode. *Biosens. Bioelectron.* **2006**, *22*, 664–669.

(11) Mercante, L. A.; Pavinatto, A.; Iwaki, L. E. O.; Scagion, V. P.; Zucolotto, V.; Oliveira, O. N., Jr.; Mattoso, L. H. C.; Correa, D. S. Electrospun Polyamide 6/Poly(allylamine hydrochloride) Nanofibers Functionalized with Carbon Nanotubes for Electrochemical Detection of Dopamine. *ACS Appl. Mater. Interfaces* **2015**, *7*, 4784–4790.

(12) McCreery, R. L. Advanced Carbon Electrode Materials for Molecular Electrochemistry. *Chem. Rev.* **2008**, *108*, 2646–2687.

(13) Yang, W.; Ratinac, K. R.; Ringer, S. P.; Thordarson, P.; Gooding, J. J.; Braet, F. Carbon Nanomaterials in Biosensors: Should You Use Nanotubes or Graphene? *Angew. Chem., Int. Ed.* **2010**, *49*, 2114–2138.

(14) Zhou, M.; Zhai, Y.; Dong, S. Electrochemical Sensing and Biosensing Platform Based on Chemically Reduced Graphene Oxide. *Anal. Chem.* **2009**, *81*, 5603–5613.

(15) Clark, J. J.; Sandberg, S. G.; Wanat, M. J.; Gan, J. O.; Horne, E. A.; Hart, A. S.; Akers, C. A.; Parker, J. G.; Willuhn, I.; Martinez, V.; Evans, S. B.; Stella, N.; Phillips, P. E. M. Chronic Microsensors for Longitudinal, Subsecond Dopamine Detection in Behaving Animals. *Nat. Methods* **2010**, *7*, 126–129.

(16) Njagi, J.; Chernov, M. M.; Leiter, J. C.; Andreescu, S. Amperometric Detection of Dopamine in Vivo with an Enzyme Based Carbon Fiber Microbiosensor. *Anal. Chem.* **2010**, *82*, 989–996.

(17) Sarter, M.; Kim, Y. Interpreting Chemical Neurotransmission in Vivo: Techniques, Time Scales, and Theories. *ACS Chem. Neurosci.* **2015**, *6*, 8–10.

(18) Wightman, R. M. Monitoring Molecules: Insights and Progress. *ACS Chem. Neurosci.* **2015**, *6*, 5–7.

(19) Banerjee, I.; Pangule, R. C.; Kane, R. S. Antifouling Coatings: Recent Developments in the Design of Surfaces That Prevent Fouling by Proteins, Bacteria, and Marine Organisms. *Adv. Mater.* **2011**, *23*, 690–718.

(20) Ostuni, E.; Chapman, R. G.; Holmlin, R. E.; Takayama, S.; Whitesides, G. M. A Survey of Structure-Property Relationships of Surfaces that Resist the Adsorption of Protein. *Langmuir* **2001**, *17*, 5605–5620.

(21) Otsuka, H.; Nagasaki, Y.; Kataoka, K. PEGylated Nanoparticles for Biological and Pharmaceutical Applications. *Adv. Drug Delivery Rev.* **2003**, *55*, 403–419.

(22) Slaughter, B. V.; Khurshid, S. S.; Fisher, O. Z.; Khademhosseini, A.; Peppas, N. A. Hydrogels in Regenerative Medicine. *Adv. Mater.* **2009**, *21*, 3307–3329.

(23) Drury, J. L.; Mooney, D. J. Hydrogels for Tissue Engineering: Scaffold Design Variables and Applications. *Biomaterials* **2003**, *24*, 4337–4351.

DOI: 10.1021/acsami.5b06526
ACS Appl. Mater. Interfaces 2015, 7, 21931–21938

(24) Sharma, S.; Johnson, R. W.; Desai, T. A. XPS and AFM Analysis of Antifouling PEG Interfaces for Microfabricated Silicon Biosensors. *Biosens. Bioelectron.* **2004**, *20*, 227−239.
(25) Iwata, R.; Suk-In, P.; Hoven, V. P.; Takahara, A.; Akiyoshi, K.; Iwasaki, Y. Control of Nanobiointerfaces Generated from Well-Defined Biomimetic Polymer Brushes for Protein and Cell Manipulations. *Biomacromolecules* **2004**, *5*, 2308−2314.
(26) Chen, S. F.; Zheng, J.; Li, L. Y.; Jiang, S. Y. Strong Resistance of Phosphorylcholine Self-Assembled Monolayers to Protein Adsorption: Insights into Nonfouling Properties of Zwitterionic Materials. *J. Am. Chem. Soc.* **2005**, *127*, 14473−14478.
(27) Iwasaki, Y.; Ishihara, K. Cell Membrane-Inspired Phospholipid Polymers for Developing Medical Devices with Excellent Biointerfaces. *Sci. Technol. Adv. Mater.* **2012**, *13*, 14.
(28) Zhang, Z.; Chen, S. F.; Chang, Y.; Jiang, S. Y. Surface Grafted Sulfobetaine Polymers via Atom Transfer Radical Polymerization as Superlow Fouling Coatings. *J. Phys. Chem. B* **2006**, *110*, 10799−10804.
(29) Cao, Z.; Jiang, S. Super-Hydrophilic Zwitterionic Poly-(carboxybetaine) and Amphiphilic Non-Ionic Poly(ethylene glycol) for Stealth Nanoparticles. *Nano Today* **2012**, *7*, 404−413.
(30) Shao, Q.; He, Y.; White, A. D.; Jiang, S. Difference in Hydration between Carboxybetaine and Sulfobetaine. *J. Phys. Chem. B* **2010**, *114*, 16625−16631.
(31) Ishihara, K.; Nomura, H.; Mihara, T.; Kurita, K.; Iwasaki, Y.; Nakabayashi, N. Why Do Phospholipid Polymers Reduce Protein Adsorption? *J. Biomed. Mater. Res.* **1998**, *39*, 323−330.
(32) Kozai, T. D. Y.; Langhals, N. B.; Patel, P. R.; Deng, X.; Zhang, H.; Smith, K. L.; Lahann, J.; Kotov, N. A.; Kipke, D. R. Ultrasmall Implantable Composite Microelectrodes with Bioactive Surfaces for Chronic Neural Interfaces. *Nat. Mater.* **2012**, *11*, 1065−1073.
(33) Fattahi, P.; Yang, G.; Kim, G.; Abidian, M. R. A Review of Organic and Inorganic Biomaterials for Neural Interfaces. *Adv. Mater.* **2014**, *26*, 1846−1885.
(34) Kumar, S. S.; Mathiyarasu, J.; Phani, K. L. Exploration of Synergism between a Polymer Matrix and Gold Nanoparticles for Selective Determination of Dopamine. *J. Electroanal. Chem.* **2005**, *578*, 95−103.
(35) Wang, W.; Xu, G.; Cui, X. T.; Sheng, G.; Luo, X. Enhanced Catalytic and Dopamine Sensing Properties of Electrochemically Reduced Conducting Polymer Nanocomposite Doped with Pure Graphene Oxide. *Biosens. Bioelectron.* **2014**, *58*, 153−156.
(36) Vreeland, R. F.; Atcherley, C. W.; Russell, W. S.; Xie, J. Y.; Lu, D.; Laude, N. D.; Porreca, F.; Heien, M. L. Biocompatible PEDOT:Nafion Composite Electrode Coatings for Selective Detection of Neurotransmitters in Vivo. *Anal. Chem.* **2015**, *87*, 2600−2607.
(37) Luo, S.-C. Conducting Polymers as Biointerfaces and Biomaterials: A Perspective for a Special Issue of Polymer Reviews. *Polym. Rev.* **2013**, *53*, 303−310.
(38) Arias-Pardilla, J.; Otero, T. F.; Yu, H.-H. Electropolymerization and Characterization of COOH-Functionalized Poly(3,4-ethylenedioxythiophene): Ionic Exchanges. *Electrochim. Acta* **2011**, *56*, 10238−10245.
(39) Luo, S.-C.; Yu, H.-h.; Wan, A. C. A.; Han, Y.; Ying, J. Y. A General Synthesis for PEDOT-Coated Nonconductive Materials and PEDOT Hollow Particles by Aqueous Chemical Polymerization. *Small* **2008**, *4*, 2051−2058.
(40) Luo, S.-C.; Kantchev, E. A. B.; Zhu, B.; Siang, Y. W.; Yu, H.-h. Tunable, Dynamic and Electrically Stimulated Lectin-Carbohydrate Recognition on a Glycan-Grafted Conjugated Polymer. *Chem. Commun.* **2012**, *48*, 6942−6944.
(41) Zhu, B.; Luo, S.-C.; Zhao, H. C.; Lin, H.-A.; Sekine, J.; Nakao, A.; Chen, C.; Yamashita, Y.; Yu, H.-H. Large Enhancement in Neurite Outgrowth on a Cell Membrane-Mimicking Conducting Polymer. *Nat. Commun.* **2014**, *5*, 9.
(42) Lee, J.-E.; Kwak, J.-W.; Park, J. W.; Luo, S.-C.; Zhu, B.; Yu, H.-h. Nanoscale Analysis of a Functionalized Polythiophene Surface by Adhesion Mapping. *Anal. Chem.* **2014**, *86*, 6865−6871.
(43) Lee, J.-E.; Luo, S.-C.; Zhu, B.; Park, J. W.; Yu, H.-h. Nanoscale Analysis of Functionalized Polythiophene Surfaces: the Effects of Electropolymerization Methods and Thermal Treatment. *RSC Adv.* **2014**, *4*, 62666−62672.
(44) Luo, S.-C.; Sekine, J.; Zhu, B.; Zhao, H.; Nakao, A.; Yu, H.-H. Polydioxythiophene Nanodots, Nonowires, Nano-Networks, and Tubular Structures: The Effect of Functional Groups and Temperature in Template-Free Electropolymerization. *ACS Nano* **2012**, *6*, 3018−3026.
(45) Lin, H.-A.; Luo, S.-C.; Zhu, B.; Chen, C.; Yamashita, Y.; Yu, H.-H. Molecular or Nanoscale Structures? The Deciding Factor of Surface Properties on Functionalized Poly(3,4-ethylenedioxythiophene) Nanorod Arrays. *Adv. Funct. Mater.* **2013**, *23*, 3212−3219.
(46) Parks, J. S.; Cistola, D. P.; Small, D. M.; Hamilton, J. A. Interactions of the Carboxyl Group of Oleic Acid with Bovine Serum Albumin: A ^{13}C NMR Study. *J. Biol. Chem.* **1983**, *258*, 9262−9269.

DOI: 10.1021/acsami.5b06526
ACS Appl. Mater. Interfaces 2015, 7, 21931−21938